Scientific African 16 (2022) e01262

Contents lists available at ScienceDirect

Scientific African

journal homepage: www.elsevier.com/locate/sciaf

Thermodynamic optimization of parallel and spiral plate heat exchangers for modified solar thermal Brayton cycle models

M. O Petinrin[a], M.J. Labiran[a], T. Bello-Ochende[b], O.M. Oyewola[a,c,*]

[a] Department of Mechanical Engineering, University of Ibadan, Ibadan, Nigeria
[b] Department of Mechanical Engineering, University of Cape Town, Cape Town, South Africa
[c] School of Mechanical Engineering, Fiji National University, Suva, Fiji

ARTICLE INFO

Article history:
Received 27 January 2022
Revised 5 April 2022
Accepted 22 June 2022

Editor: DR B Gyampoh

Keywords:
Brayton cycle
Parallel plate heat exchanger
Optimisation
Spiral plate heat
Exchanger

ABSTRACT

The receiver and heat exchangers in a Solar Thermal Brayton Cycle (STBC) have been the main sources of exergy loss. Duct profiles used in the heat exchange process have been observed to possess varying degrees of heat transfer effectiveness. To this end, the effects of the elliptical, circular and rectangular absorber tubes are investigated on three variants of the dual serial-regenerative STBC models employing reheater, intercooler, or in a combined arrangement. Also, the impact of the parallel plate heat exchanger (PPHE) and spiral plate heat exchangers (SPHE) on irreversibility is investigated. The particle swarm algorithm (PSA), a stochastic optimization tool is used for the minimization of irreversibilities within the cycle and optimization of the geometric parameters of the STBC components. The largest irreversibility loss on a component-basis is observed on the receiver. The rectangular absorber system for the receiver has the least irreversibility loss compared to other profiles studied, though, a higher internal to external irreversibility ratio was noticed. Improved exergy use via the dual regenerative system was observed on all models with reductions of 22% and 15% in irreversibility obtained from the receiver and recuperator respectively. In addition, the SPHE produced less irreversibilities compared to the PPHE system and this could be attributed to its large surface area available for heat transfer. An optimal second law efficiency of 62% and 74% on the PPHE and SPHE STBC systems, respectively is achieved at around a pressure ratio of 2.2. The dual serial-regenerative system without reheats and intercooling has the advantage of optimal energy available and efficient exergy use followed by the combined system.

Introduction

Effective and efficient power generating systems are required by the world to meet its growing energy needs. The efficiency of a conventional stand-alone Brayton cycle has been observed to be low. Design modifications with subsequent addition of components has been made to improve it [27]. Reheating and Regeneration are amongst methods used to in-

* Corresponding author.
E-mail address: oooyewola001@gmail.com (O.M. Oyewola).

https://doi.org/10.1016/j.sciaf.2022.e01262

Nomenclature

a	Longer side of channel width-m
A	Area-m^2
B	Shorter side of channel-m
c	Specific heat capacity-J/kgK
D	Dish diameter-m
d	Channel/dish diameter-m
Ep	Dish concentrator error-rad
E	Exergy-J
$\dot{E}$	Exergy rate-W
eff	Effectiveness
F	Darcy friction factor
g	Acceleration due to gravity-m/s^2
h	Convection heat transfer-W/m^2K
H	Height – Recuperator-m
I	Irreversibility rate-W
K	Boltzman's constant
k	Thermal conductivity-W/mK
l	Length-m
$\dot{m}$	Mass flow rate-kg/s
n	Number of fins/ recuperator channels
Nu	Nusselt Number
P	Pressure-Pa
Pr	Prandtl number
Q	Heat Energy-J
$\dot{Q}$	Heat energy rate-W
r	Pressure ratio
Re	Reynolds number
S	Entropy-J/K
t	Thickness of separator plate-m
T	Temperature-K
T^*	Apparent sun temperature-K
U	Overall heat transfer coefficient-W/mK
V	Velocity-m/s
W	Work-J

Greek Symbols

η	Efficiency
μ	Dynamic viscosity-kg/ms
ρ	Density-kg/m^3
ν	Kinematic viscosity-m^2/s

Subscripts

1	First/Initial state
2	Second/Final state
atm	Atmospheric
avg	Average
b	Boundary
C	Cold stream
$Conc$	Concentrator
$Conv$	Convection
D	Destruction
E	Exit/Outlet
Ext	External
F	Fuel
gen	Generation
h	Hot stream
i	Inlet

int	Internal
loss	Loss due to convection and conduction
Net	Net
o	Outlet
rad	Radiation
rec	Receiver/Recuperator
T	Turbine
Th	Thermal
v	Constant volume

AMbbreviations

CSP	Concentrated Solar-Thermal Technologies
EGM	Entropy Generation Minimization
HP	High Pressure-Pa
LT	Low Temperature-K
HTR	High Temperature Recuperator
LP	Low Pressure-Pa
LT	Low Temperature-K
LTR	Low Temperature Recuperator
NTU	Number of transfer units
PPHE	Parallel Plate Heat Exchanger
RIT	Recuperator Inlet Temperature-K
SPHE	Spiral Plate Heat Exchanger
SLA	Second Law Analysis
STBC	Solar Thermal Brayton Cycle
TIT	Turbine Inlet Temperature-K

crease the TIT which improves the cycle's efficiency. Notwithstanding, the system is still been plagued by high irreversibility formation [5].

The second law analysis (SLA) which incorporates the first and second law of thermodynamics provides a reliable method to detect, quantify and minimize irreversibility generation. ([15,17,23]; W. [30]). Studies revealed that the SLA was used to identify the compressor and optical errors in the concentrator as the component/parameters responsible for the loss of exergy [3,21]. The entropy generation minimization (EGM) method uses the principles of heat transfer, mass transfer and fluid flow in analyzing thermodynamic cycles which is important in determining the operating and geometric parameters of components while minimizing exergy loss and optimizing the net work output [1,6,8].

In integrating solar receivers to the Brayton cycle, Le Roux et al. [14] determined the optimum points of selected turbomachines in four weather conditions in Pretoria using EGM. The study opined that deployment of the solar thermal Brayton cycle (STBC) is possible in varying weather conditions with mass flow rate controls and optimized turbomachine geometries. In like manner, EGM was used to select the intercooled variant of a regenerative STBC model as the preferred of three twin-shaft STBC designs studied [18]. Jansen et al. [10] studied the impact of dual connection of recuperators on the reduction of irreversibilites in open and closed loop STBCs. The study showed a greater efficiency of the dual over the single recuperative system.

In the STBC cases studied, higher exergy losses were seen at the receiver and recuperator. Opportunities to reduce irreversibilities in the recuperative system exist with the choice of the cross sectional profiles for the absorber tubes. Jebasingh et al. [11] observed that the efficiency of the collector system was improved with elliptical as against circular cross sectional absorber tubes. Shah [25] observed circular cross sections has reduced surface areas for flow, lower heat transfer coefficient and larger pressure drops which encourage the formation of irreversibilities thereby reducing the exergetic efficiency of the system [7,26].

Efficient recuperation is crucial to improved efficiency and performance for power cycles and counter flow recuperative systems have been found to be effective in STBC systems [2,25]. The parallel plate heat exchanger (PPHE) has been used in the study of a simple case and analysis revealed that it is the second most dominant source of exergy loss ([18]; Le Roux et al., 2014). The SPHE unlike the PPHE circulates cold fluid from its outer section through its rolled plates and exits it through the center while the hot fluid flows likewise from the alternate direction [4]. The SPHE provides a large heat surface area amid a reduction in fouling in ensuring an improved heat transfer and would be applied in this study [22].

In this paper, EGM is performed on three variants of a STBC model with a dual serial recuperative system. With an HTR and LTR in place, it attempts to improve waste heat recovery with dual recuperation as against a single recuperative means and compare the effects of the spiral and parallel plate heat exchangers in improving the TIT. The solar receiver absorber tubular would be varied using the elliptical, rectangular and circular geometry. The particle swarm algorithm, a stochastic optimization tool will be used for the cycle's optimization. It is intended that the study will provide further knowledge needed in the optimization and deployment of STBC for small scale power generation.

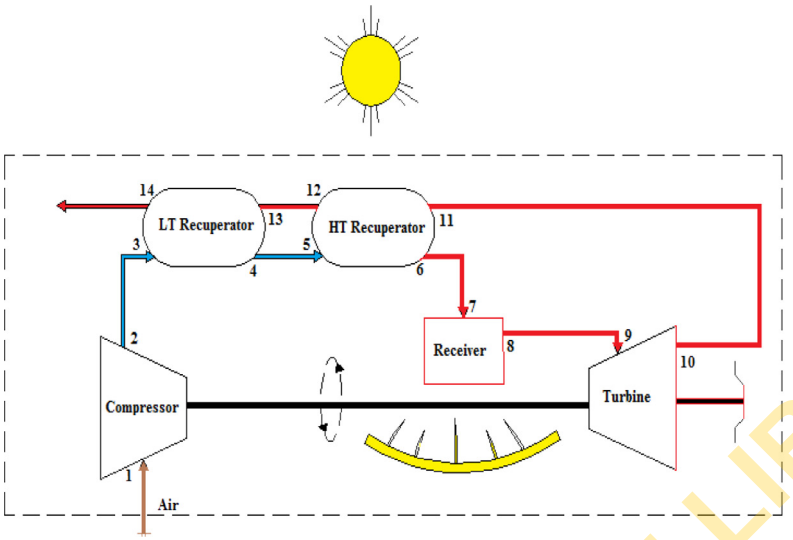

Fig. 1. Schematic shows Model 1 with Recuperation only.

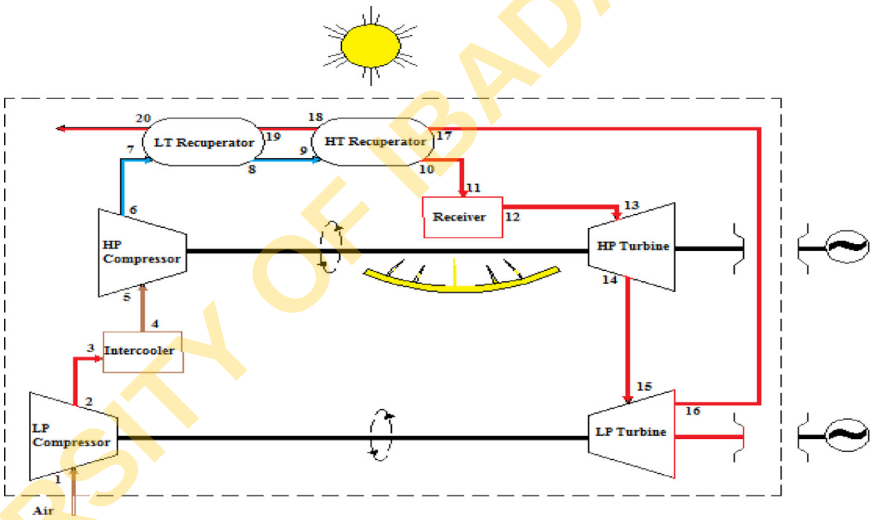

Fig. 2. Schematic shows Model 2 with Intercooling and Recuperation.

Cycle Description

Figs. 1-3 shows the schematic representation of the modified STBC cycle to be analyzed. The models drawn each includes the HTR and LTR system and are derived based on component arrangements within the cycle.

Model 1: STBC with recuperation only.

Model 2: STBC with Intercooling and recuperation.

Model 3: STBC with, Intercooling, Reheat and recuperation.

Components used in the STBC design includes dish-mounted modified cavity receiver, counter-flow recuperators (PPHE/SPHE), intercooler and automotive turbochargers configured as turbomachines.

The system is considered to have air at its ambient temperature of 30K and pressure of 101325Pa as its cycle's working fluid. All heat transfer process are assumed to be steady while a constant high temperature reservoir is used as source of heat addition exergy. For simplicity in calculations, a 2K temperature drop is assumed along the duct connecting components and working fluid mass flow rate is constant.

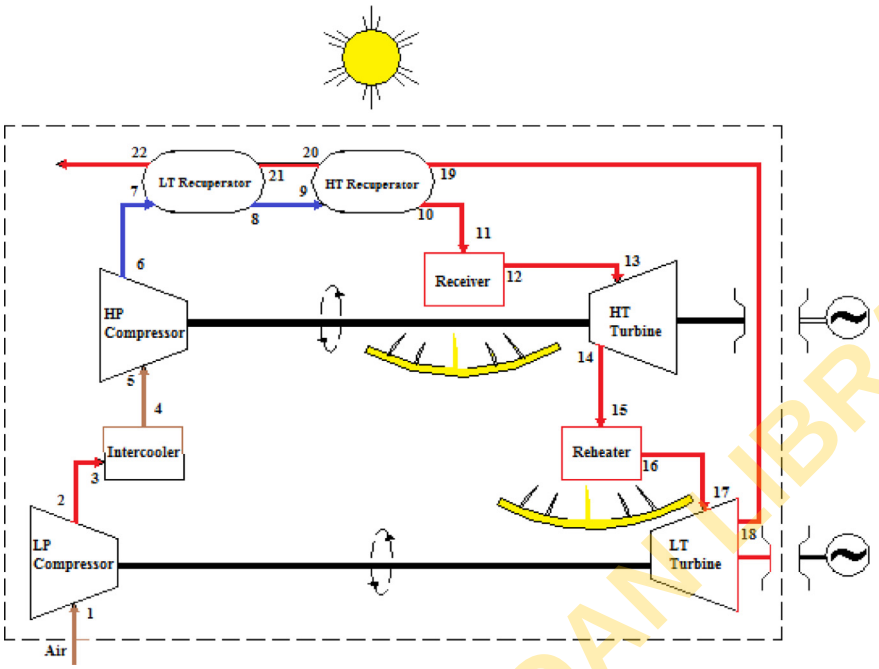

Fig. 3. Schematic shows Model 3 with Intercooling, Reheat, and Recuperation.

Objective function

For a steady flow system, Jubeh, [12] showed that the exergy balance is derived as (1),

$$\dot{E}_{heat} - \dot{W} + \dot{E}_{mass} - \dot{X}_{dest} = 0 \tag{1}$$

The parameters in Eq. (1), E_{heat}, W, E_{mass} and $X_{dest.}$ are defined as exergy transfer by heat, mass, work and lost respectively with $X_{dest.}$ obtained from (2).

$$\dot{X}_{dest} = T_o \sum \dot{S}_{gen} \tag{2}$$

The irreversibility generated in the system is a function of the surrounding temperature and the entropy generated through all the components in the cycle and is obtained using Guoy-Stodola theorem as seen in Eq. (2). The component by component entropy generation rate is calculated using Eq. (3). Hence, the total entropy generated by the cycle is calculated as the sum of the entropy generated by all the components of the cycle.

$$\dot{S}_{gen} = \dot{m}c_p In\left(\frac{T_{out}}{T_{in}}\right) - \dot{m}RIn\left(\frac{P_{out}}{P_{in}}\right) - \frac{1}{T}\sum Q_{cv} \tag{3}$$

The total work derived from the power cycle is calculated as;

$$\dot{W}_{net} = \dot{Q}_{net} + \dot{m}c_p(T_{in} - T_{out}) - \dot{m}T_o c_p In\left(\frac{T_{in}}{T_{out}}\right) - \dot{X}_{dest} \tag{4}$$

The objective function is taken as Eq. (4), and its parameters are changed to suit other models to be investigated.

Solar receiver and reheater

Parabolic concentrator is used to converge the solar rays from the sun to the receiver for isothermal heating of the working fluid. Several receiver types have been investigated and suggested for use in solar concentrating technologies (CST). The modified cavity type shown in Fig. 5 is preferred to the semi-cavity and cavity receiver variant as it produces lower convection losses. A wall to cavity area ratio of eight (8) is adopted as it was observed to produce minimum convection losses compared to other design studied [24].

The receiver is made with copper tubes as it has a high thermal conductivity and a melting point of 1200K which is higher relative to most metals [16]. The simulation is performed with circular, rectangular and elliptical absorber tubes as shown in Fig. 4. For simplicity in calculations losses due to convection and radiation in the receiver are considered to be equal [10].

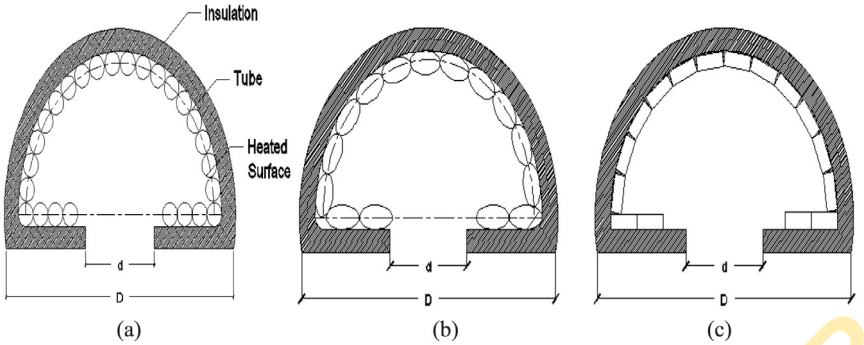

Fig. 4. Modified cavity receiver with (a) circular, (b) elliptical and (c) rectangular tubing system [24]

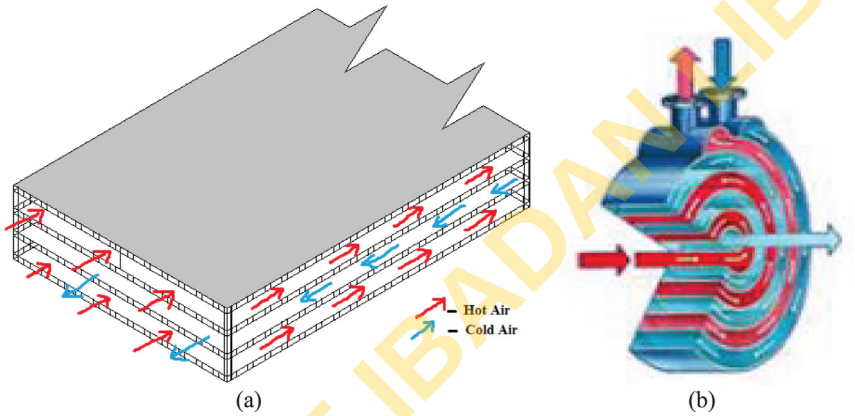

Fig. 5. Schematic of the (a) PPHE and (b) SPHE cross-section [13,20].

Hence, the entropy generated in the receiver is calculated using Eq. (5);

$$\dot{S}_{gen,rec} = -\frac{Q^*}{T^*} + \frac{\dot{Q}_o}{T_o} + \dot{m}c_p In\frac{T_e}{T_i} - \dot{m}RIn\frac{P_e}{P_i} \tag{5}$$

Recuperator

The component is used for recovering waste heat from the gas exhausted from the turbine and an optimal heat transfer area exists which improve the thermal efficiency [5]. Using the PSA, component geometries that dissuade high formation of irreversibilities will be selected. The PPHE and SPHE systems to be considered on the STBC design are shown in Fig. 5.

The entropy generation in the recuperator is obtained from Eq. (6);

$$\dot{S}_{gen,reg} = \dot{m}c_p In\left[\frac{T_{c,e}T_{h,e}}{T_{c,i}T_{h,i}}\left(\frac{P_{c,e}P_{h,e}}{P_{c,i}P_{h,i}}\right)^{\frac{(1-k)}{k}}\right] + \frac{\dot{m}c_p(T_{m,reg} - T_o)}{T_o} \tag{6}$$

The temperature from the cold outlet of the selected heat exchanger is calculated as;

$$T_{c,out} = T_{c,in} - \varepsilon_n\left(T_{h,in} - T_{c,in}\right) \tag{7}$$

The Intercooling Unit

The cross-flow design of an intercooler, shown in Fig. 6, used by Meas and Bello-Ochende, [18] is employed for its simplicity as its design is oriented to aid the flow of surrounding air by natural convection through its vertical channels.

To obtain the entropy generated by the intercooler, Eq. (8) is used

$$\dot{S}_{gen,\text{intercooler}} = \dot{m}\left[c_{p,hic}In\frac{T_e}{T_i} - RIn\frac{P_e}{P_i} + c_{p,hic}\frac{(T_i - T_e)}{T_{sc,ic}}\right] \tag{8}$$

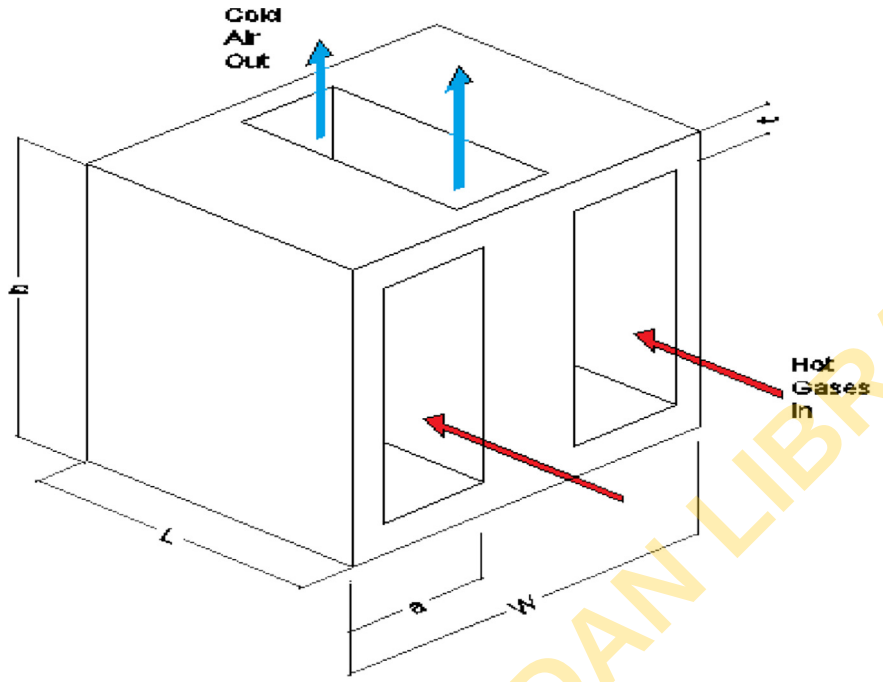

Fig. 6. Schematic representation of the cross-flow intercooler.

Turbine and Compressor Components

Automotive turbomachines are used to simulate the turbine and compressor parameters. The mass flow rate through the compressor of the microturbine is taken as the mass flow rate of the system. The Garrett range of turbomachines was used in this work because its work range is readily obtainable [9].

The exergy loss from the turbine and compressor is evaluated using Eq. (9) [12].

$$\dot{S}_{gen,turbomachine} = \dot{m}\left[c_p In\frac{T_e}{T_i} - RIn\frac{P_e}{P_i}\right] \tag{9}$$

The subscripts, i and e denotes inlet and exit of thermodynamic parameters.

Ducts connecting STC Components

A 2K differential is used to obtain the temperature at the duct nodes connecting the components. Its corresponding rate of entropy generation is obtained via Eq. (10)

$$\dot{S}_{gen,duct} = \dot{m}\left[c_p In\frac{T_e}{T_i} - RIn\frac{P_e}{P_i} + \frac{c_p T_{drop}}{T_o}\right] \tag{10}$$

Nodal Pressure and Temperature Relationship

Values of the pressure and temperature at the commencement of the cycle process is taken as 1 atm and 300K respectively. The pressure and temperature at selected nodes in the system will be obtained using thermodynamic relationship for calculation of the rate of entropy generation from the individual components.

Pressure and temperature drop at the ducts will be obtained via Eqs. (11-12)

$$T_e = T_i - T_{drop} \tag{11}$$

$$P_e = P_i - (\Delta P_{e,i} * P_i) \tag{12}$$

At the turbomachinery components, pressure and temperature are obtained via equations (13–14)

$$P_e = rP_i \tag{13}$$

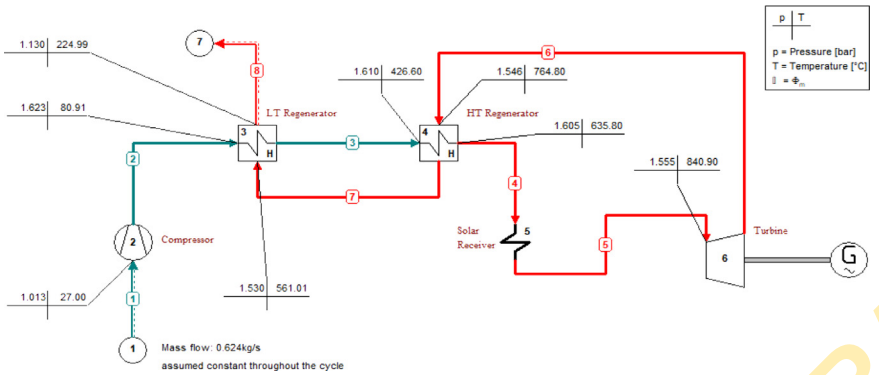

Fig. 7. STBC Model 1 Simulation performed using ASIMPTOTE Cycle Tempo.

$$T_e = T_i\left(1 + \left(\left(r_c^{\frac{k-1}{k}} - 1\right)/\eta_{comp}\right)\right) \tag{14}$$

Similar formulation would be used for other cases after the removal of appropriate components unique to the arrangement. For the calculations, thermal conductivity, k, fouling factor, R_f, and plate thickness, t, for the recuperator and intercooler are taken as 401 W/mK, 0.001 and 1 mm.

Numerical Optimization

The optimization process commences with the formulation of the objective function and constraints developed with respect to the design [29]. As against the deterministic optimization method, the study leverages the robustness of the stochastic optimization algorithm [28]. The entropy generation parameter, S_{gen}, is to be minimised subjected to the constraints imposed on the STBC components. The code begins by generating a swarm of particles which represents the geometric parameters of components which is weighted by the design constraints. Values defined as "personal best" are then stored upon evaluating the objective function. The iteration continues until a global best value is obtained. Nabab, [19] summed up the algorithm in equation (105-106) as;

$$V_{i,j}^{k+1} = w\left(V_{i,j}^{k}\right) + c_1 r_1\left(Pbest_{i,j}^{k}\right) + c_2 r_2\left(Gbest_{j}^{k} - X_{i,j}^{k}\right) \tag{15}$$

Where $X_{i,j}^{k+1} = X_{i,j}^{k} + V_{i,j}^{k+1}$(16)

Parameters, c_1 and c_2 defined as acceleration factors take the value of 2, while the inertia weight, w is set at 0.9.

Program Validation

The codes used for simulating the thermodynamic, geometric and PSO algorithm was written using the MATLAB program. Optimized geometric parameters obtained for the spiral recuperator in the MATLAB simulation was used to obtain the nodal pressure and temperature of the STBC Model 1 using Cycle Tempo by ASIMPTOTE as shown in Fig. 7. An observation of the results as depicted in Fig. 8 shows a good correlation of both results at the start nodes and only begins to deviates as it approaches the heat exchanger components. A deviation of -0.3 to 6.9% was obtained with an optimal value of 19% recorded at the exhaust node.

Results and discussions

Optimizations of the three models were performed using the particle swarm-based optimizer tool modelled in MATLAB with definite collector dish radii and design properties obtained from the Garrett turbomachines. The results obtained from the simulation are analyzed as follows;

Turbine Inlet Temperature and Recuperator Inlet Temperature

The TIT is amongst the parameter that determines the amount of expansion work available from the turbine. An increased TIT almost equivocally leads to an increased network output. A comparison of the TIT generated via the STBC variants studied is presented in Fig. 9-11. Data obtained from a single regenerative system studied by Meas [18] was included in the analysis (Fig. 11). It is deduced that the TIT values for the dual recuperative system are higher compared to the single system. Model 2 is observed to generate higher TIT at lower pressure ratios. An optimal TIT value is obtained with the double serial regenerative SPHE STBC variant at a pressure ratio of 1.8 to 2.0 across all models. It is also observed that

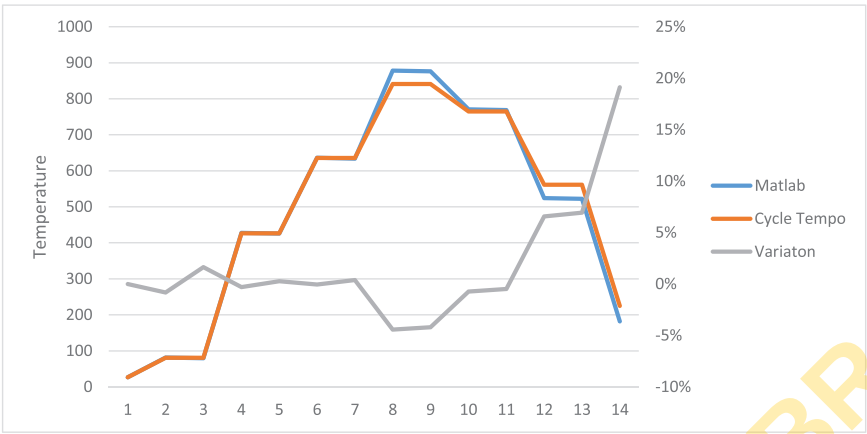

Fig. 8. Comparison of the temperature results for the Matlab and the Cycle Tempo at the system nodal points.

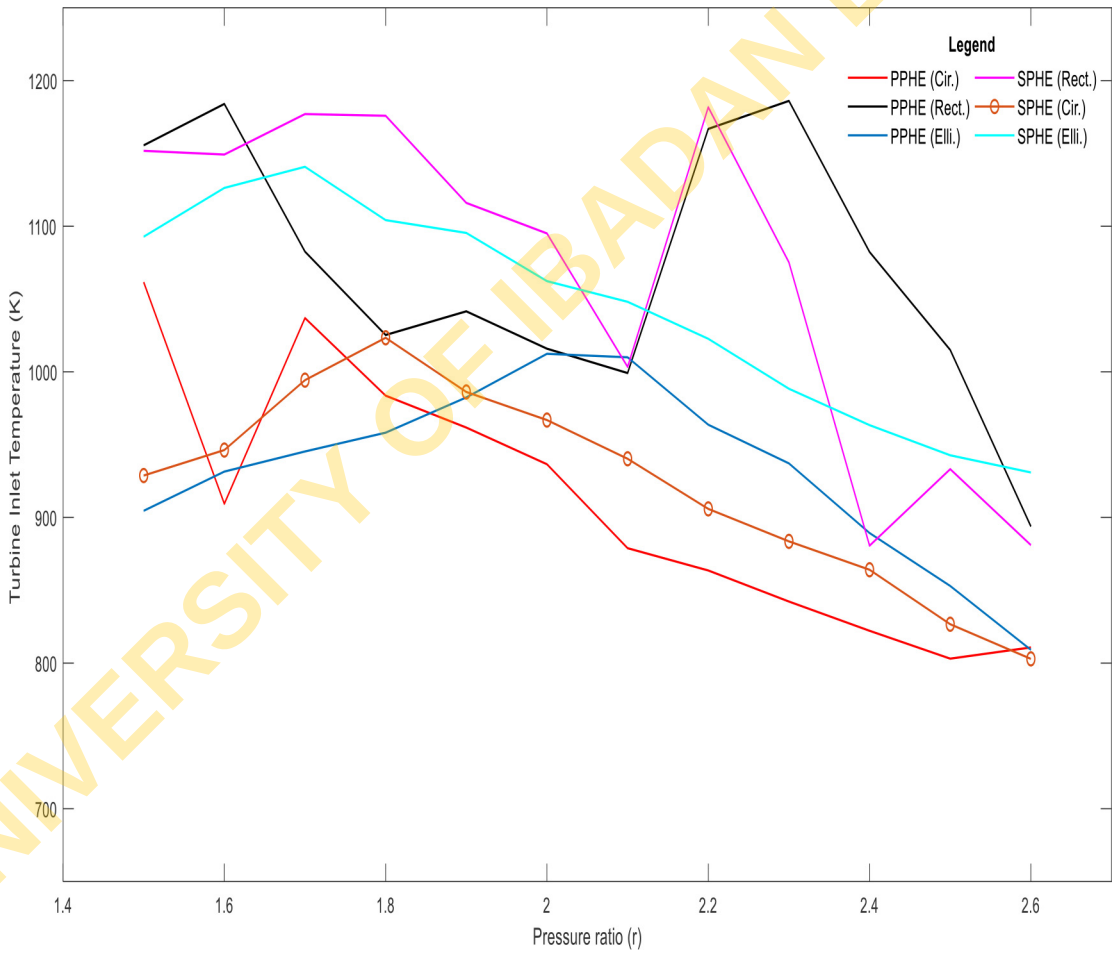

Fig. 9. Plot showing the TIT values obtained for Model 1 using the PPHE and SPHE recuperators incorporating differing receiver/reheater channel profiles.

the SPHE performed better across the pressure ranges compared to the PPHE variant with the elliptical and rectangular tube configurations delivering higher TIT values. RIT values for the SPHE is also found to be higher than all other models studied, however it is further observed that the amount of energy available for waste heat recovery reduces with increase in turbomachine pressure ratio.

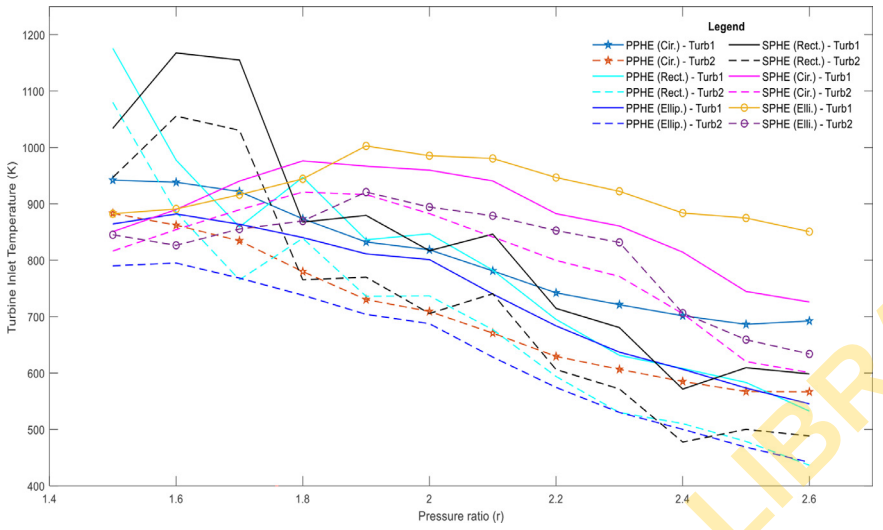

Fig. 10. Plot showing the TIT values obtained for Model 2 using the PPHE and SPHE recuperators incorporating differing receiver/reheater channel profiles.

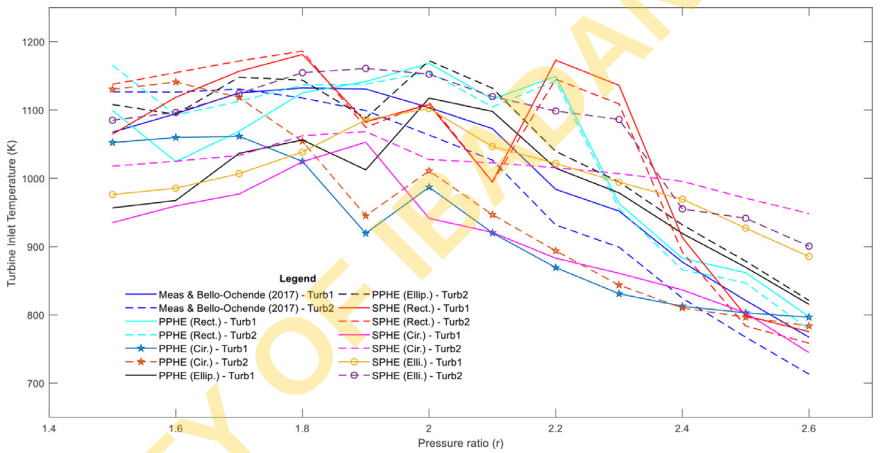

Fig. 11. Plot showing the TIT values obtained for Model 3 using the PPHE and SPHE recuperators incorporating differing receiver/reheater channel profiles (reference case included for comparison).

Net Work Output

The amount of work derived from the turbine across the mass flow range for all variants studied is shown in Figs. 12-13. Increased work output is obtained in all the models studied with the SPHE system. At higher pressure ratios however, the net work obtainable is slightly lower than the alternate PPHE system. Optimal net work is observed at a mass flow range of 2.2 – 2.3kg/s, hence a significantly proportional relationship is observed between the TIT and the net work output.

Irreversibility Distribution

Figs. 14-15 shows the distribution of irreversibility generation in the system components at maximum net work output for Model 1, 2 and 3. It can be deduced that the receiver contributes significantly to the formation of irreversibility within the system.

Systems with the least irreversibility generation from the receiver include the SPHE for Model *1* and *2* while the PPHE system achieves this feat in Model 3. An approximate reduction in exergy loss of 22% and 11% from the receiver is observed in the former and latter respectively.

First and Second Law Efficiency

Based on the work out and heat input to all STBC configurations studied, the first and second law efficiencies were determined.

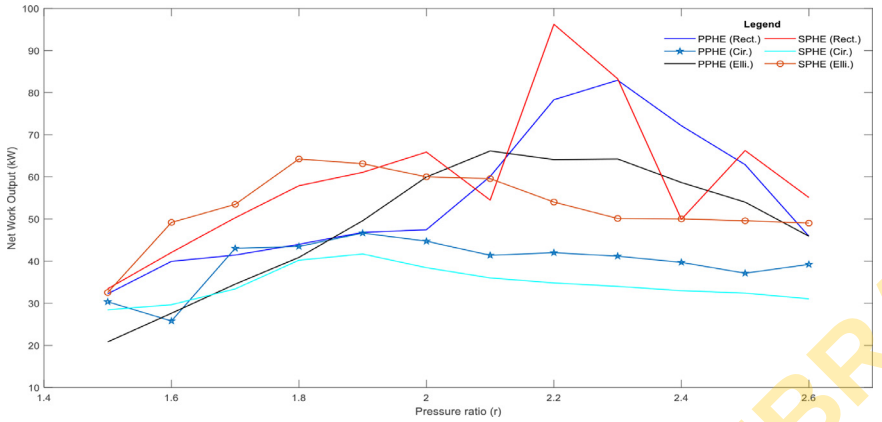

Fig. 12. Plot showing Model 1 net work output of the double regenerative STBC obtained over the pressure ratio using the PPHE and SPHE recuperators with differing receiver channel profiles.

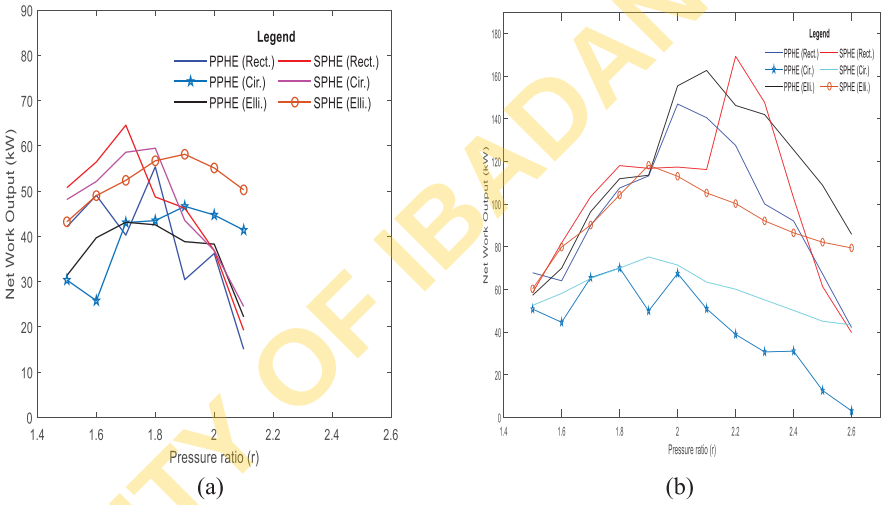

Fig. 13. Plot showing network output of the double regenerative STBC using the PPHE and SPHE recuperators incorporating differing receiver channel profiles for Model (a) 2 (b) 3.

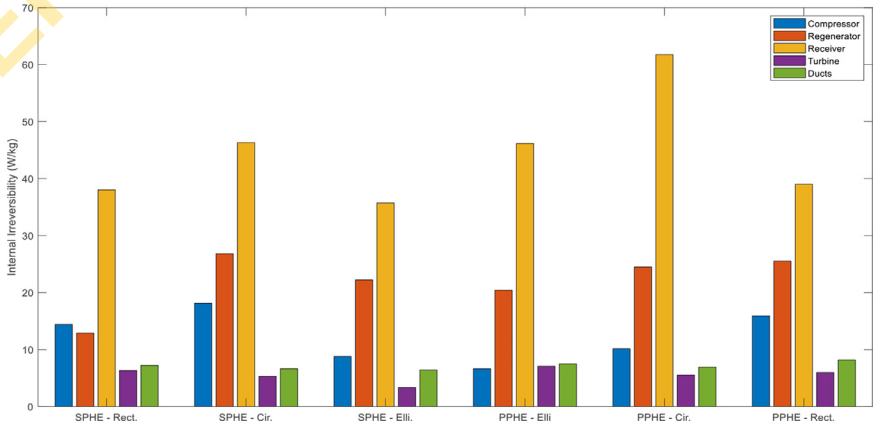

Fig. 14. Chart showing the distribution of irreversibility (at max work output) on Model 1.

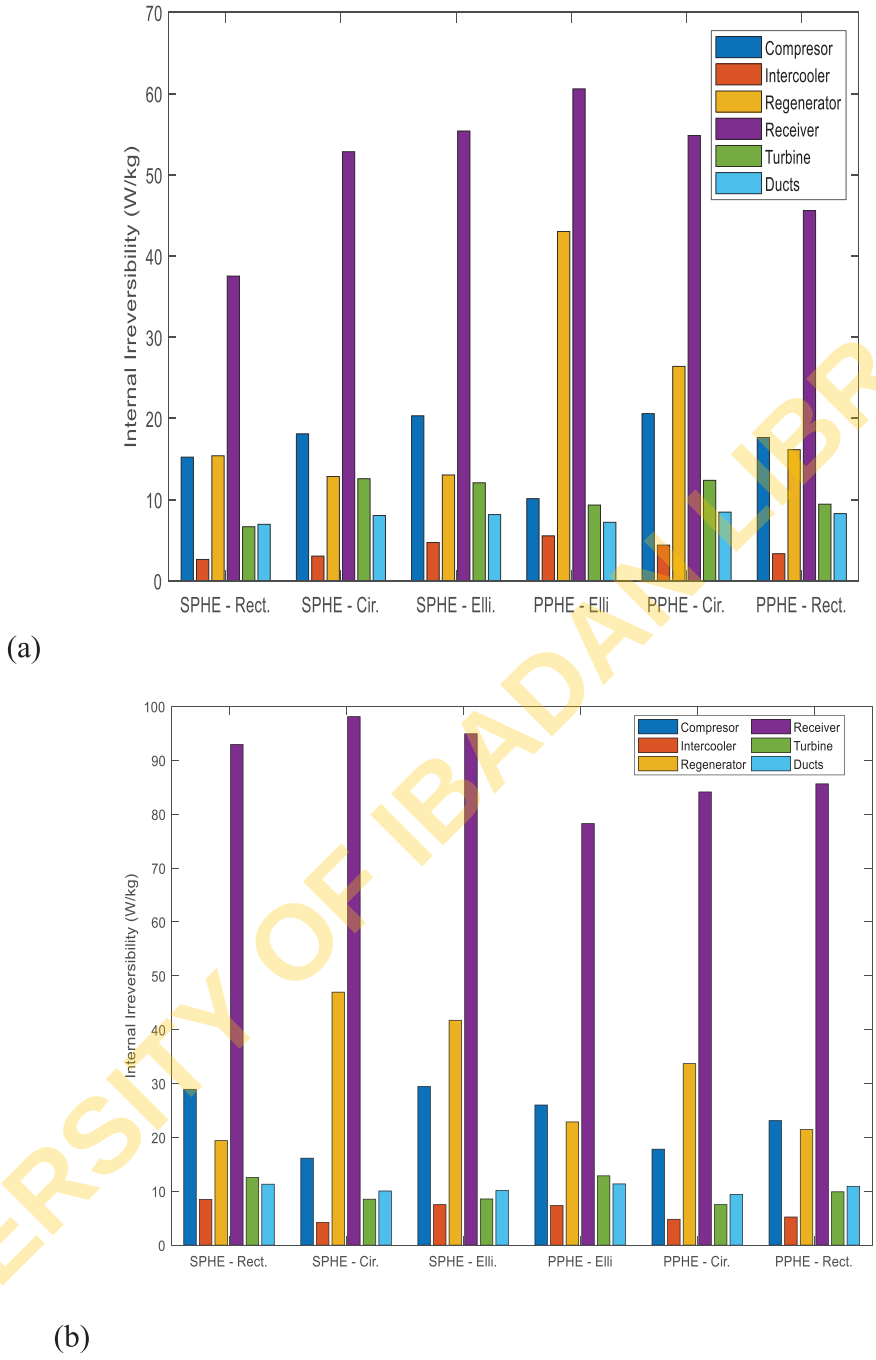

Fig. 15. Chart showing irreversibility distribution at max work output (a) Model 2 (b) Model 3.

From Fig. 16, it is observed that a strong positive correlation exists between the first and the second law efficiencies. Optimal efficiencies are noted for all models studied at about a pressure ratio of 1.9 to 2.2 except the circular channel type which hovers at a ratio of approximately 1.8. With reference to Figs. 9, 10 and 11, efficiency occurs at regions where TIT peaks. An improved second law efficiency is observed with the SPHE STBC and Model 1 accounts for improved exergy use amongst the cases studied. It was also noted that the efficiency obtained via rectangular absorber channels were better compared to the elliptical and circular in that order.

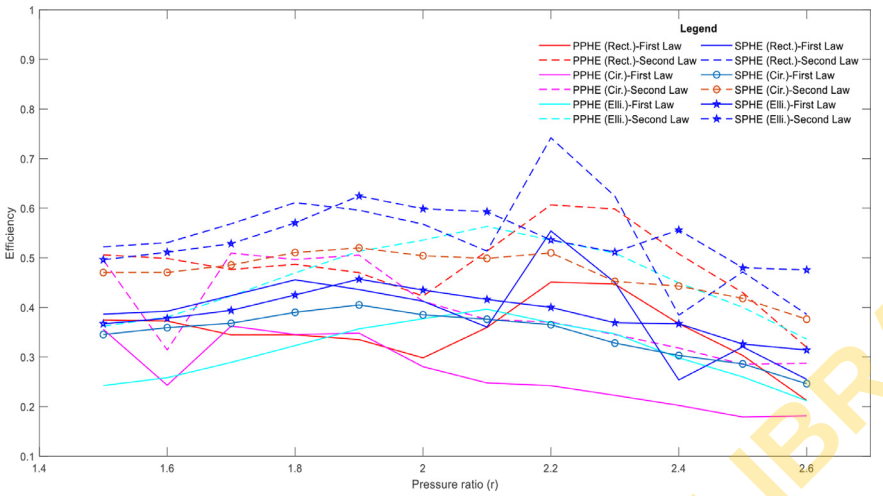

Fig. 16. Plot shows the first and second law efficiencies of STBC models.

Conclusion

The performance of a serial regenerative solar thermal Brayton cycle was studied using entropy generation minimization method. The network output was defined as the objective function and a stochastic optimization tool - particle swarm algorithm was used to minimize the exergy generated within the system. As studies have indicated, the solar receiver and recuperator are two components with the highest values of entropy generated. This necessitated the modelling of the former with varying cross-sectional profiles and introduction of the SPHE with the PPHE. Three recuperative STBC case studies employing the reheat and intercooling methods exclusively and in combination were modelled.

The rectangular profile was observed to reduce exergy loss in the receiver and reheater the most compared to other absorber profiles. It was also observed that the geometric profiles of the receiver were minimized with the elliptical absorber profiles. The circular absorber profiles had optimal receiver sizes amidst the most exergy loss. First and second law efficiencies were improved on the rectangular profiles for the parallel plate heat exchanger, however it increased further with the application of the spiral plate exchanger system. The increased total heat surface area obtainable from the latter was influential to reducing the exergy loss from the regenerative unit. Of all the models studied, the simple dual serial recuperative system had an improved exergy use.

The impact of the combined recuperative STBC system should be compared with experiments and subjected to further analysis in the near future. These areas could be in the use of ductless receivers which would reduce complexities arising from installation, operation and maintenance; optimization of duct lengths. In addition, thermoeconomic study performed on the system. This would be required to foster the energy de-carbonisation scheme through widespread adoption of CSP technologies in Africa especially now that efficient thermal energy storage systems could be incorporated to ensure all round usage of the system. The introduction of the SPHE into the STBC will ensure that the energy source is more compact and can be deployed in remote locations.

Declaration of Competing Interest

The paper titled “Thermodynamic optimisation of Parallel and Spiral Plate Heat Exchangers for Modified Solar Thermal Brayton Cycle Models” is joint authorship carried out by M.O. Petinrin, M. J. Labiran, T. Bello-Ochende and O.M. Oyewola. All the authors read and approved the article. There is no conflict of interest among the authors.

References

[1] A.S. Adavbiele, Optimization of thermofluid systems with second law, Int. J. Eng. Res. Afr. 1 (2010) 67–80, doi:10.4028/www.scientific.net/jera.1.67.
[2] M.H. Ahmadi, M. Alhuyi Nazari, R. Ghasempour, F. Pourfayaz, M. Rahimzadeh, T Ming, A review on solar-assisted gas turbines, Energy Sci. Eng. 6 (6) (2018) 658–674, doi:10.1002/ese3.238.
[3] A.M. Bahman, E.A. Groll, Second-law analysis to improve the energy efficiency of environmental control unit, in: 16th International Refrigeration and Air Conditioning Conference at Purdue, 2016, pp. 1–10.
[4] L. Canizalez Dávalos, E. Murrieta Luna, M. Alberto Rodríguez Ángeles, J. Cruz Delgado, V, Designing spiral plate heat exchangers to extend its service and enhance the thermal and hydraulic performance, Low-Temp. Technol. (2020) 1–16, doi:10.5772/intechopen.85345.
[5] H. Feng, C. Cai, L. Chen, Z. Wu, G. Lorenzini, Constructal design of a shell-and-tube condenser with ammonia-water working fluid, Int. Commun. Heat Mass Transf. 118 (2020) 104867, doi:10.1016/j.icheatmasstransfer.2020.104867.
[6] H. Feng, L. Chen, Z. Wu, Z. Xie, International Journal of Heat and Mass Transfer Constructal design of a shell-and-tube heat exchanger for organic fluid evaporation process, Int. J. Heat Mass Transf. 131 (2019) 750–756, doi:10.1016/j.ijheatmasstransfer.2018.11.105.
[7] H. Feng, L. Chen, S. Xia, International Journal of Heat and Mass Transfer Constructal design for disc-shaped heat exchanger with maximum thermal efficiency, Int. J. Heat Mass Transf. 130 (2019) 740–746, doi:10.1016/j.ijheatmasstransfer.2018.11.003.

[8] H. Feng, L. Chen, Z. Xie, W. Tang, Y. Ge, Multi-objective constructal design for a marine boiler considering entropy generation rate and power consumption, Energy Rep. 8 (2022) 1519–1527, doi:10.1016/j.egyr.2021.12.071.
[9] GarrettTurbomachine Data Sheet 2019, 2019.
[10] E. Jansen, T. Bello-ochende, J.P. Meyer, Integrated solar thermal Brayton cycles with either one or two regenerative heat exchangers for maximum power output, Energy 86 (2015) 737–748, doi:10.1016/j.energy.2015.04.080.
[11] V.K. Jebasingh, G.M. Joselin Herbert, Numerical simulation of elliptical absorber tube in parabolic trough collector for better heat transfer, Indian J. Sci. Technol. 8 (24) (2015) 1–7, doi:10.17485/ijst/2015/v8i24/80165.
[12] N.M. Jubeh, Exergy analysis and second law efficiency of a regenerative Brayton cycle with isothermal heat addition, Entropy 7 (3) (2005) 172–187, doi:10.3390/e7030172.
[13] W. Le Roux, T. Bello-Ochende, J. Meyer, Minimization and Optimum Distribution of Entropy Generation for Maximum Net Power Output of the Small--Scale Open and Direct Solar Thermal Brayton Cycle, 2009 *2008*.
[14] W. Le Roux, T. Bello-Ochende, J.P. Meyer, Operating conditions of an open and direct solar thermal Brayton cycle with optimised cavity receiver and recuperator, Energy 36 (10) (2011) 6027–6036, doi:10.1016/j.energy.2011.08.012.
[15] T.S. Lee, Second-Law analysis to improve the energy efficiency of screw liquid chillers, Entropy 12 (3) (2010) 375–389, doi:10.3390/e12030375.
[16] R. Loni, E.A. Asli-ardeh, B. Ghobadian, E. Bellos, W.G. Le Roux, Numerical comparison of a solar dish concentrator with different cavity receivers and working fl uids, J. Clean. Prod. 198 (2018) 1013–1030, doi:10.1016/j.jclepro.2018.07.075.
[17] S. Mamalis, A. Babajimopoulos, D. Assanis, C. Borgnakke, A modeling framework for second law analysis of low-temperature combustion engines, Int. J. Engine Res. 15 (6) (2014) 641–653, doi:10.1177/1468087413512312.
[18] Meas, M. R., & Bello-Ochende, T. (2017). Thermodynamic design optimisation of an open air recuperative twin-shaft solar thermal Brayton cycle with combined or exclusive reheating and intercooling. *Energy Convers. Manag.*, 148, 770–784. https://doi.org/10.1016/j.enconman.2017.06.043
[19] M. Nabab, Particle Swarm Optimization: Algorithm and its Codes in MATLAB, ResearchGate 1 (2016) 8–12, doi:10.13140/rg.2.1.4985.3206.
[20] M. Nunez, L. Davalos, A. Fuentes, Alternative design approach for spiral plate heat exchangers, Chemic. Eng. Trans. 5 (2007) 183–188.
[21] R.V. Padilla, A. Fontalvo, G. Demirkaya, A. Martinez, A.G. Quiroga, Exergy analysis of parabolic trough solar receiver, Appl. Therm. Eng. 67 (1–2) (2014) 579–586, doi:10.1016/j.applthermaleng.2014.03.053.
[22] M. Picón-Núñez, L. Canizalez-Dávalos, G. Martínez-Rodríguez, G.T. Polley, Shortcut design approach for spiral heat exchangers, Food Bioprod. Process. 85 (4 C) (2007) 322–327, doi:10.1205/fbp07073.
[23] J. Sarkar, Second law analysis of supercritical CO2 recompression Brayton cycle, Energy 34 (9) (2009) 1172–1178, doi:10.1016/j.energy.2009.04.030.
[24] K.N. Sendhil, K.S. Reddy, Comparison of receivers for solar dish collector system, Energy Convers. Manage. 49 (4) (2008) 812–819, doi:10.1016/j.enconman.2007.07.026.
[25] R.K. Shah, Compact heat exchangers for microturbines, in: International Conference of Enhanced, Compact and Ultra-Compact Heat Exchangers: Science, Engineering and Technology, 2005, pp. 247–257. *September*.
[26] O.P. Sharma, S.C. Kaushik, K. Manjunath, Thermodynamic analysis and optimization of a supercritical CO2regenerative recompression Brayton cycle coupled with a marine gas turbine for shipboard waste heat recovery, Therm. Sci. Eng. Progress 3 (2017) 62–74, doi:10.1016/j.tsep.2017.06.004.
[27] J. Vecchiarelli, J.G. Kawall, J.S. Wallace, Analysis of a concept for increasing the efficiency of a brayton cycle via isothermal heat addition, Int. J. Energy Res. 21 (2) (1997) 113–127, doi:10.1002/(SICI)1099-114X(199702)21:2(113::AID-ER219)3.0.CO;2-5.
[28] X. Wang, M. Damodaran, Comparison of deterministic and stochastic optimization algorithms for generic wing design problems, J. Aircr. 37 (5) (2000) 929–932, doi:10.2514/2.2695.
[29] H.J. Yang, K.S. Hwang, C.J. Lee, Stochastic optimization of a natural gas liquefaction process considering seawater temperature variation based on particle swarm optimization, Ind. Eng. Chem. Res. 57 (6) (2018) 2200–2207, doi:10.1021/acs.iecr.7b04546.
[30] W. Zhang, L. Chen, F. Sun, C. Wu, Second-law analysis and optimisation for combined Brayton and inverse Brayton cycles, Int. J. Ambient Energy 28 (1) (2007) 15–26, doi:10.1080/01430750.2007.9675020.